Deep-learning-based image segmentation for uncommon ischemic stroke

From infants to adults

Zoetmulder, R.

Publication date
2023

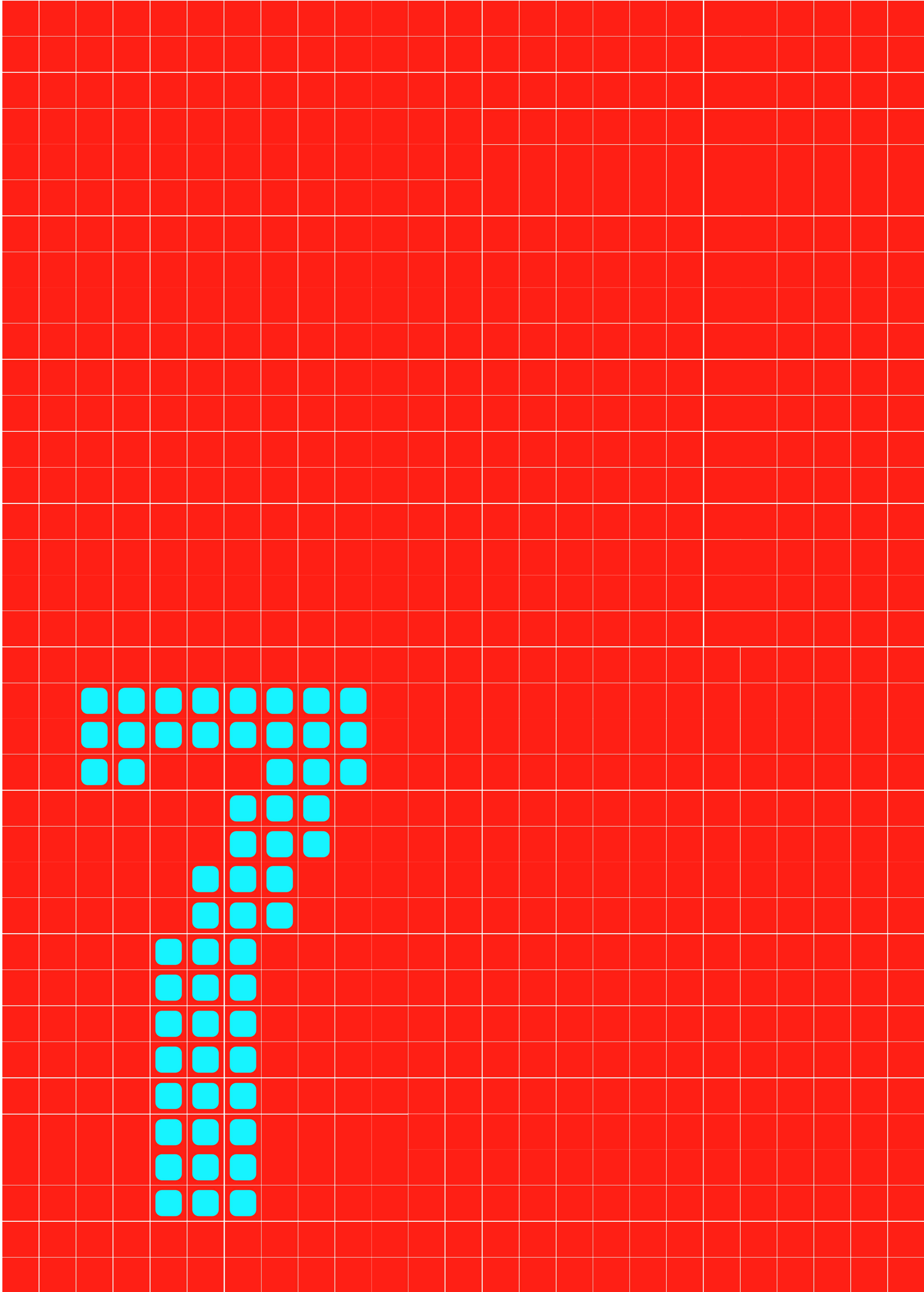

Chapter 7

General Discussion

General Discussion

Contributions to stroke research

An important aspect of modern stroke research involves analysing segmentation-based image characteristics derived from scans, such as thrombus volume and lesion volume. However, manual annotation of image data is labor- and time-intensive. Hence, there is an interest to automate the segmentation process. Currently, deep learning is the best available technique to automate image segmentation. A limiting factor to the development, application, and evaluation of deep learning-based segmentation methods is that they often require a large amount of data. Less common sub-types of stroke that have few available data have not yet benefited from deep learning-based segmentation. Therefore, the primary focus of this thesis was to investigate, develop, and evaluate deep learning-based algorithms for the segmentation of images of sub-types of stroke that have few data available.

Final lesion volume has been proposed as an outcome measure in acute stroke reperfusion clinical trials [258]. Subsequently, follow-up NCCT was shown to have a strong association to functional outcome in anterior circulation stroke [237; 260]. Due to the scarcity of available data in posterior circulation stroke, the association between final lesion volume and functional outcome is understudied. The study in chapter 3 has shown that deep learning can be used to automatically segment lesions due to a posterior circulation large vessel occlusion on follow-up NCCT of adult patients. The developed algorithm can be used to study associations between segmentation-based lesion characteristics, such as lesion volume, and functional outcome. The method can reduce the annotation burden by providing automatic segmentations. However, due to the low spatial overlap the resulting automatically generated segmentations should be inspected and, if necessary, manually corrected.

Thrombus image characteristics have been associated with treatment outcome in anterior circulation stroke in adult patients by prior studies. The studied thrombus image characteristics for anterior circulation stroke are perviousness, density, and length [236; 238; 242; 245; 249; 254; 255]. However, one study showed that the only thrombus characteristic that is associated with functional outcome in posterior circulation stroke is thrombus length [240]. A limitation of current applications of thrombus length, perviousness, and density assessment is that they are derived from Region-of-Interest (ROI) markers in the proximal, medial, and distal parts of the thrombus rather than complete segmentations. Prior research has already shown that thrombus segmentations provide more information than ROI markers [256]. Segmentations have been used in conjunction with techniques from radiomics to extract thrombus characteristics in patients with anterior circulation stroke. These characteristics were found to be more predictive than thrombus length, permeability, and density [253]. The algorithm developed in 4 makes it easier to test for these associations by reducing the annotation burden in posterior stroke clinical trials and registries that involve adult patients.

Effectiveness of novel neuro-protective and neuro-regenerative treatments, such as recombinant tissue erythropoietin [235] and mesenchymal stromal cells [234], can be tested by comparing brain tissue volumes between each hemisphere on baseline and follow-up scans. This is possible due to most cases of stroke being confined to a single hemisphere. If treatments are effective, patients with perinatal arterial ischemic stroke treated with neuro-protective and neuro-regenerative agents should have a similar volume for all tissue classes in both hemispheres due to more brain tissue retention and growth after the stroke. Moreover, the volume of the ischemic region can be added to the analysis to control for possible interactions between lesion size and treatment. However, annotating each scan manually would require approximately a week of work per scan. The network instances developed in chapter 5 reduce the manual annotation burden by automating the segmentation process. A limitation of the presented network instances is that the resulting segmentations may require manual inspection and correction before being used in an analysis, specifically of the ischemic region on the baseline scans. Moreover, due to limited variability in the training dataset, generalizations to scans from other MRI machines and protocols may be limited. Hence, further development is required before possible clinical use of our network instances.

Contributions to medical image segmentation research

With the exception of the brain-tissue segmentation algorithms introduced in chapter 5, all methods make use of some variant of transfer learning and build on the findings in chapter 2. In chapter 2, we demonstrated that applying transfer learning to medical segmentation tasks yields the best results if the source domain and task are similar to the target domain and task. Hence, pre-training on automatically generated segmentations adds little cost relative to self-supervised pre-training, but has greater benefit if the data is similar.

Accurately segmenting small objects in medical scans is a difficult task due to the large class imbalance, limited available data, and variable presentation. A standard UNet approach applied to the entire scan volume results in a large number of false positive segmentations. By localizing small objects prior to segmenting small objects, false positive segmentation can be reduced. Various methods that localize a structure in a medical scan prior to segmenting it have been developed in earlier work [239; 244; 247; 250; 257; 261; 262]. An often used method of localization is by using a bounding box regression [239; 241; 247; 261]. Bouget et al. combined a 2D Mask R-CNN in conjunction with a 2D U-Net to localize and segment mediastinal lymph nodes and anatomical structures in the mediastinal area [239]. The 2D bounding boxes are converted to 3D by combining consecutive 2D bounding boxes. Liang et al. used a different method to combine bounding boxes to localize and segment organs at risk in head and neck images [247]. Their method combined features extracted from axial, coronal or sagittal slices as input. By using a voting method the features were combined before bounding box regression and segmentation. Zhang et al. used a fixed-size bounding box located around the esophagus to improve segmentation [261]. The bounding box location was found by using previously segmented structures that are close to the oesophagus. De Vos et al. used a neural network to predicted the probability that a structure was visible on slices from the three anatomical planes [241]. Using the starting location and ending location on each anatomical plane, a bounding box was constructed. Using a 3D bounding box would not have

7

been the best way of detecting thrombi in the posterior circulation, which was described in chapter 4. This is due to the variable orientation that the thrombus has, which would cause a bounding box to be much larger than required in order to contain the entire thrombus. This may result in a larger amount of false positive thrombus localization and segmentation.

Future research directions

Posterior Circulation Stroke

The results from our automated posterior stroke lesion segmentation method can be used to estimate the overall infarcted volume. However, the severity of clinical deficit not only depends on the total volume but may also depend on the specific affected substructures. A study has already shown that lesion volume in specific structures is associated with worse outcome 90 days after the stroke than other structures in anterior circulation stroke [243]. In posterior circulation stroke, hypo-attenuation of specific structures is predictive of worse outcome [252]. Similarly, future research could focus on developing a model to quantify the volume of these hypo-attenuated structures of the brain in the posterior region.

One interesting research direction that could be explored to improve the quantification of the thrombus characteristics, arterial filling and stenosis detection during a posterior circulation stroke is deep learning-based artery centerline tracking. Wolterink et al. developed a method to track the coronary arteries [259]. The automatically extracted centerlines can help visualization of the artery by straightening it using Multi-Planar Reformatting (MPR). Subsequent research used MPR straightened arteries to localize plaque type and the clinical significance of any stenosis [263]. Likewise, for posterior stroke such an approach could be used to segment the thrombus, stenosis, and the lumen of the involved arteries.

Deep learning approaches that involve segmentation in the posterior fossa are hampered by CT image artifacts, such as beam hardening. An interesting challenge could be to make deep learning-based methods more robust to CT imaging artifacts. Specifically, a data augmentation method could be devised to mimic CT artifacts during training. Such data augmentation techniques already exist for MRI [246; 251] and CT .

Perinatal Arterial Ischemic Stroke

The methods that were developed in chapter 5 segment brain tissue in patients that suffer or have suffered from perinatal arterial ischemic stroke. These methods currently rely on two separate instances of a deep neural network; one for term and one for three month follow-up scans. We developed separate network instances for term and follow-up scans for two reasons. First, the degree of myelination increases as the infant develops. This causes the appearance of the brain on T2 scans acquired at term versus follow-up to differ. Second, during the term scan the DWI shows the hypo-perfused area in the brain. Hence, this sequence is added to the network instance trained at term but not at follow-up. Future trials and registries for this type of stroke may, however, have imaging performed at other stages of development of the infant. Because the brain changes rapidly during the first year of life, generalization of the network instances to images acquired at other stages of development cannot be assumed. Therefore, a more general method to segment brain tissue on MRI scans acquired during the first year of life, which has already been developed for scans of patients not afflicted by severe pathology [248], is of interest for brains afflicted by perinatal arterial ischemic stroke.

Bibliography

[234] L. M. Baak, N. Wagenaar, N. E. van der Aa, F. Groenendaal, J. Dudink, M. L. Tataranno, U. Mahamuud, L. S. de Vries, F. van Bel, M. J. N L Benders, C. Development, R. K. Jellema, L. M. Baak, N. Wagenaar, N. E. van der Aa, F. Groenendaal, J. Dudink, M. Luisa Tataranno, U. Mahamuud, C. H. Verhage, R. M. J C Eijsermans, L. S. Smit, R. K. Jellema, T. R. de Haan, H. J. ter Horst, W. P. de Boode, S. J. Steggerda, H.-J. Prins, C. G. de Haar, L. S. de Vries, F. van Bel, C. J. Heijnen, C. H. Nijboer, and M. J. N L Benders. Feasibility and safety of intranasally administered mesenchymal stromal cells after perinatal arterial ischaemic stroke in the Netherlands (PASSIoN): a first-in-human, open-label intervention study. *The Lancet Neurology*, 21(6):528–536, 6 2022.

[235] M. J. Benders, N. E. Van Der Aa, M. Roks, H. L. Van Straaten, I. Isgum, M. A. Viergever, F. Groenendaal, L. S. De Vries, and F. Van Bel. Feasibility and safety of erythropoietin for neuroprotection after perinatal arterial ischemic stroke. *The Journal of pediatrics*, 164(3), 2014.

[236] A. B. Bilgic, R. Gocmen, E. M. Arsava, and M. A. Topcuoglu. The Effect of Clot Volume and Permeability on Response to Intravenous Tissue Plasminogen Activator in Acute Ischemic Stroke. *Journal of Stroke and Cerebrovascular Diseases*, 29(2):104541, 2 2020.

[237] A. M. Boers, I. Jansen, l. F. M Beenen, T. Devlin, L. san roman, J. hoe heo, M. Ribó, S. Brown, M. Almekhlafi, D. Liebeskind, J. Teitelbaum, h. F. Lingsma, W. van Zwam, P. Cuadras, M. Beaumont, M. M. Brown, a. J. Yoo, r. J. van Oostenbrugge, B. K. Menon, G. Donnan, J. louis Mas, Y. B. W M roos, C. Oppenheim, A. van der lugt, r. J. Dowling, M. D. Hill, A. Davalos, T. Moulin, N. Agrinier, a. M. Demchuk, D. K. Lopes, L. aja rodríguez, D. W. J Dippel, B. V. Campbell, P. J. Mitchell, F. Al-ajlan, T. Jovin, J. Madigan, g. W. Albers, S. Soize, F. Guillemin, V. K. Reddy, S. Bracard, J. Blasco, K. W. Muir, R. Nogueira, P. M. White, M. Goyal, s. M. Davis, H. Marquering, and c. B. M Majoie. Association of follow-up infarct volume with functional outcome in acute ischemic stroke:

7

a pooled analysis of seven randomized trials. *J NeuroIntervent Surg*, 10:1137–1142, 2018.

[238] J. Borst, O. A. Berkhemer, E. M. Santos, A. J. Yoo, M. Den Blanken, Y. B. Roos, E. Van Bavel, W. H. Van Zwam, R. J. Van Oostenbrugge, H. F. Lingsma, A. Van Der Lugt, D. W. Dippel, H. A. Marquering, and C. B. Majoie. Value of Thrombus CT Characteristics in Patients with Acute Ischemic Stroke. *AJNR. American journal of neuroradiology*, 38(9):1758–1764, 9 2017.

[239] D. Bouget, A. Jørgensen, G. Kiss, H. O. Leira, and T. Langø. Semantic segmentation and detection of mediastinal lymph nodes and anatomical structures in CT data for lung cancer staging. *International Journal of Computer Assisted Radiology and Surgery*, 14(6):977–986, 3 2019.

[240] A. A. E. Bruggeman, J. Brouwer, . Nerea, A. Terreros, N. Boodt, S. J. Den Hartog, A. Pirson, . Ludo, F. M. Beenen, P.-J. Van Doormaal, R. J. Van Oostenbrugge, J. Staals, . Wim, H. Van Zwam, . Wouter, J. Schonewille, . Lucianne, C. M. Langezaal, J.-A. Vos, . Aad Van Der Lugt, . Diederik, W. J. Dippel, J. M. Coutinho, . Yvo, B. W. E. M. Roos, H. A. Marquering, B. J. Emmer, . Charles, and B. L. M. Majoie. Thrombus Imaging Characteristics and Outcomes in Posterior Circulation Stroke Patients Treated With EVT. *Stroke: Vascular and Interventional Neurology*, 2(3), 5 2022.

7

[241] B. D. De Vos, J. M. Wolterink, P. A. De Jong, T. Leiner, and M. A. Viergever. ConvNet-Based Localization of Anatomical Structures in 3D Medical Images.

[242] B. G. Dutra, M. L. Tolhuisen, H. C. Alves, K. M. Treurniet, M. Kappelhof, A. J. Yoo, I. G. Jansen, D. W. Dippel, W. H. Van Zwam, R. J. Van Oostenbrugge, A. J. Da Rocha, H. F. Lingsma, A. Van Der Lugt, Y. B. Roos, H. A. Marquering, and C. B. Majoie. Thrombus Imaging Characteristics and Outcomes in Acute Ischemic Stroke Patients Undergoing Endovascular Treatment. *Stroke*, 50(8):2057–2064, 8 2019.

[243] M. Ernst, A. M. Boers, A. Aigner, O. A. Berkhemer, A. J. Yoo, Y. B. Roos, D. W. Dippel, A. Van Der Lugt, R. J. Van Oostenbrugge, W. H. Van Zwam,

J. Fiehler, H. A. Marquering, and C. B. Majoie. Association of Computed Tomography Ischemic Lesion Location with Functional Outcome in Acute Large Vessel Occlusion Ischemic Stroke. *Stroke*, 48(9):2426–2433, 9 2017.

[244] K. He, X. Cao, Y. Shi, D. Nie, Y. Gao, and D. Shen. Pelvic Organ Segmentation Using Distinctive Curve Guided Fully Convolutional Networks. *IEEE Transactions on Medical Imaging*, 38(2):585–595, 2 2019.

[245] M. Kappelhof, M. L. Tolhuisen, K. M. Treurniet, B. G. Dutra, H. Alves, G. Zhang, S. Brown, K. W. Muir, A. Davalos, Y. B. Roos, J. L. Saver, A. M. Demchuk, T. G. Jovin, S. Bracard, B. C. Campbell, A. Van Der Lugt, F. Guillemin, P. White, M. D. Hill, D. W. Dippel, P. J. Mitchell, M. Goyal, H. A. Marquering, and C. B. Majoie. Endovascular Treatment Effect Diminishes with Increasing Thrombus Perviousness: Pooled Data from 7 Trials on Acute Ischemic Stroke. *Stroke*, 52(11):3633–3641, 11 2021.

[246] N. Khalili, N. Lessmann, E. Turk, N. Claessens, R. d. Heus, T. Kolk, M. A. Viergever, M. J. Benders, and I. Išgum. Automatic brain tissue segmentation in fetal MRI using convolutional neural networks. *Magnetic Resonance Imaging*, 64:77–89, 12 2019.

[247] S. Liang, K. H. Thung, D. Nie, Y. Zhang, and D. Shen. Multi-View Spatial Aggregation Framework for Joint Localization and Segmentation of Organs at Risk in Head and Neck CT Images. *IEEE Transactions on Medical Imaging*, 39(9):2794–2805, 9 2020.

[248] P. Moeskops, M. A. Viergever, A. M. Mendrik, L. S. De Vries, M. J. Benders, and I. Isgum. Automatic Segmentation of MR Brain Images with a Convolutional Neural Network. *IEEE Transactions on Medical Imaging*, 35(5):1252–1261, 5 2016.

[249] M. Mokin, M. Waqas, J. Fifi, R. De Leacy, D. Fiorella, E. I. Levy, K. Snyder, R. Hanel, K. Woodward, I. Chaudry, A. T. Rai, D. Frei, J. E. Delgado Almandoz, M. Kelly, A. S. Arthur, B. W. Baxter, J. English, I. Linfante, K. M. Fargen, A. Turk, A. H. Siddiqui, and J. Mocco. Clot perviousness is associated with first pass success of aspiration thrombectomy in the COMPASS trial. *Journal of NeuroInterventional Surgery*, 13(6):509–514, 6 2021.

[250] J. Noothout, E. Postma, S. Boesveldt, B. D. de Vos, P. Smeets, and I. Išgum. Automatic segmentation of the olfactory bulbs in MRI. In *115961J*, volume 11596, page 51. SPIE-Intl Soc Optical Eng, 2 2021.

[251] F. Pérez-García, R. Sparks, and S. Ourselin. TorchIO: A Python library for efficient loading, preprocessing, augmentation and patch-based sampling of medical images in deep learning. *Computer Methods and Programs in Biomedicine*, 208, 9 2021.

[252] V. Puetz, P. N. Sylaja, S. B. Coutts, M. D. Hill, I. Dzialowski, P. Mueller, U. Becker, G. Urban, C. O'Reilly, P. A. Barber, P. Sharma, M. Goyal, G. Gahn, R. Von Kummer, and A. M. Demchuk. Extent of hypoattenuation on CT angiography source images predicts functional outcome in patients with basilar artery occlusion. *Stroke*, 39(9):2485–2490, 9 2008.

[253] W. Qiu, H. Kuang, J. Nair, Z. Assis, M. Najm, C. McDougall, B. McDougall, K. Chung, A. T. Wilson, M. Goyal, M. D. Hill, A. M. Demchuk, and B. K. Menon. Radiomics-Based Intracranial Thrombus Features on CT and CTA Predict Recanalization with Intravenous Alteplase in Patients with Acute Ischemic Stroke. *American Journal of Neuroradiology*, 40(1):39–44, 1 2019.

[254] E. M. Santos, J. W. Dankbaar, K. M. Treurniet, A. D. Horsch, Y. B. Roos, L. J. Kappelle, W. J. Niessen, C. B. Majoie, B. Velthuis, and H. A. Marquering. Permeable Thrombi Are Associated with Higher Intravenous Recombinant Tissue-Type Plasminogen Activator Treatment Success in Patients with Acute Ischemic Stroke. *Stroke*, 47(8):2058–2065, 8 2016.

[255] E. M. Santos, H. A. Marquering, M. D. Den Blanken, O. A. Berkhemer, A. M. Boers, A. J. Yoo, L. F. Beenen, K. M. Treurniet, C. Wismans, K. Van Noort, H. F. Lingsma, D. W. Dippel, A. Van Der Lugt, W. H. Van Zwam, Y. B. Roos, R. J. Van Oostenbrugge, W. J. Niessen, and C. B. Majoie. Thrombus Permeability Is Associated with Improved Functional Outcome and Recanalization in Patients with Ischemic Stroke. *Stroke*, 47(3):732–741, 3 2016.

[256] E. M. Santos, A. J. Yoo, L. F. Beenen, O. A. Berkhemer, M. D. den Blanken, C. Wismans, W. J. Niessen, C. B. Majoie, and H. A. Marquering. Observer

variability of absolute and relative thrombus density measurements in patients with acute ischemic stroke. *Neuroradiology*, 58(2):133–139, 2 2016.

[257] S. Wang, K. He, D. Nie, S. Zhou, Y. Gao, and D. Shen. CT male pelvic organ segmentation using fully convolutional networks with boundary sensitive representation. *Medical Image Analysis*, 54:168–178, 5 2019.

[258] S. J. Warach, M. Luby, G. W. Albers, R. Bammer, A. Bivard, B. C. Campbell, C. Derdeyn, J. J. Heit, P. Khatri, M. G. Lansberg, D. S. Liebeskind, C. B. Majoie, M. P. Marks, B. K. Menon, K. W. Muir, M. W. Parsons, A. Vagal, A. J. Yoo, A. V. Alexandrov, J.-C. Baron, D. J. Fiorella, A. J. Furlan, J. Puig, P. D. Schellinger, and M. Wintermark. Acute Stroke Imaging Research Roadmap III Imaging Selection and Outcomes in Acute Stroke Reperfusion Clinical Trials. *Stroke*, 47(5):1389–1398, 2016.

[259] J. M. Wolterink, R. W. Hamersvelt, M. A. Viergever, T. Leiner, and I. Išgum. Coronary artery centerline extraction in cardiac CT angiography using a CNN-based orientation classifier. *Medical Image Analysis*, 51:46–60, 1 2019.

[260] S. F. Zaidi, A. Aghaebrahim, X. Urra, M. A. Jumaa, B. Jankowitz, M. Hammer, R. Nogueira, M. Horowitz, V. Reddy, and T. G. Jovin. Final infarct volume is a stronger predictor of outcome than recanalization in patients with proximal middle cerebral artery occlusion treated with endovascular therapy. *Stroke*, 43(12):3238–3244, 12 2012.

[261] L. Zhang, J. Zhang, P. Shen, G. Zhu, P. Li, X. Lu, H. Zhang, S. A. Shah, and M. Bennamoun. Block Level Skip Connections across Cascaded V-Net for Multi-Organ Segmentation. *IEEE Transactions on Medical Imaging*, 39(9):2782–2793, 9 2020.

[262] Y. Zhao, H. Li, S. Wan, A. Sekuboyina, X. Hu, G. Tetteh, M. Piraud, and B. Menze. Knowledge-Aided Convolutional Neural Network for Small Organ Segmentation. *IEEE Journal of Biomedical and Health Informatics*, 23(4):1363–1373, 7 2019.

[263] M. Zreik, R. W. Van Hamersvelt, J. M. Wolterink, T. Leiner, M. A. Viergever, and I. Išgum. A Recurrent CNN for Automatic Detection

and Classification of Coronary Artery Plaque and Stenosis in Coronary CT Angiography. *IEEE Transactions on Medical Imaging*, 38(7):1588–1598, 7 2019.

7